SANDIA REPORT SAND85—0321 • Unlimited Release • UC—70
Printed September 1985

Mineralogy in the Waste Isolation Pilot Plant (WIPP) Facility Stratigraphic Horizon

Carol L. Stein

Prepared by
Sandia National Laboratories
Albuquerque, New Mexico 87185 and Livermore, California 94550
for the United States Department of Energy
under Contract DE-AC04-76DP00789

Issued by Sandia National Laboratories, operated for the United States Department of Energy by Sandia Corporation.

Printed in the United States of America
Available from
National Technical Information Service
U.S. Department of Commerce
5285 Port Royal Road
Springfield, VA 22161

NTIS price codes
Printed copy: A03
Microfiche copy: A01

SAND85-0321
Unlimited Release
Printed September 1985

Distribution
Category UC—70

Mineralogy in the Waste Isolation Pilot Plant (WIPP) Facility Stratigraphic Horizon

Carol L. Stein
Earth Sciences Division
Sandia National Laboratories
Albuquerque, NM 87185

Abstract

Forty-six samples were selected for this study from two cores, one extending 50 ft up through the roof of the WIPP facility and the other penetrating 50 ft below the facility floor. These samples, selected from approximately every other foot of core length, represent the major lithologies present in the immediate vicinity of the WIPP facility horizon: "clean" halite, polyhalitic halite, argillaceous halite, and mixed polyhalitic-argillaceous halite. Samples were analyzed for non-NaCl mineralogy by determining weight percents of water- and EDTA-insoluble residues, which were then identified by x-ray diffraction. In general, WIPP halite contains at most 5 wt% non-NaCl residue. The major mineral constituents are quartz, magnesite, anhydrite, gypsum, polyhalite, and clays. Results of this study confirm that, in previous descriptions of WIPP core, trace mineral quantities have been visually overestimated by approximately an order of magnitude.

Acknowledgments

Gautam Sarkar, a graduate student in the Geology Department at the University of New Mexico, provided the weight-percent data and the x-ray diffraction analyses of the non-NaCl mineral residues. His attention to detail throughout both phases of this time-consuming project is gratefully acknowledged. In addition, I thank Klaus Keil of the Institute of Meteoritics, the UNM Geology Department, for his assistance and for many helpful discussions. The manuscript was much improved by the reviews provided by David J. Borns of Division 6331 and by Klaus Keil.

Contents

Figures

Tables

Mineralogy in the Waste Isolation Pilot Plant (WIPP) Facility Stratigraphic Horizon

Introduction

As part of the Waste Isolation Pilot Plant (WIPP) continued geotechnical studies, Sandia National Laboratories (SNL) has been charged with the task of producing a detailed characterization of the geologic interval in the immediate vicinity of the WIPP facility. Preliminary work toward this end was begun in 1983 with the Site and Preliminary Design Validation (SPDV) report. The SPDV work includes a comprehensive mineralogical analysis of 43 rock samples taken at or near the facility horizon. These samples consisted primarily of grab samples taken from the excavation face as mining proceeded, and of selected samples from cores taken from some of the excavated rooms. These samples were processed for their mineralogical components by a method described in detail in the final SPDV report (Stein, 1983) and summarized elsewhere in this report. The end result was a compilation of data that quantitatively describe the non-NaCl portion of the host halite in the general stratigraphic vicinity of the WIPP facility horizon.

An important conclusion from this set of data is that, up until the time of the SPDV report, visual estimates of the non-NaCl components were incorrect by as much as an order of magnitude or more. The appearance of the Salado halite can be deceptive, especially when it contains small quantities of very fine-grained, disseminated polyhalite or clay minerals. In summary, from the SPDV work it was learned that WIPP halite contains an average maximum of 5 wt% non-NaCl mineralogy, except in the cases of units such as anhydrites and clay seams.

This information was, in turn, used to revise some of the ongoing work directed toward predicting long-term creep behavior of the salt around the excavated cavity. However, one shortcoming of the SPDV work concerned the distribution of the sample locations of the analyzed material. It was felt that a more comprehensive body of data could be obtained by using samples from precisely known locations and could be collected on a more tightly spaced grid. Moreover, the plan for the sampling program that was ultimately adopted also provided for samples to be taken simultaneously for rock mechanics testing by W. Wawersik (SNL, Division 1542). Lastly, executing this program provided a set of reference samples for the purpose of making more quantitative visual comparisons of rock samples and a suite of archived core that will remain on file at the WIPP site for future reference.

Methods

The samples selected for this study were taken primarily from two cores, each ~ 50 ft long and 4½ in. diameter, that were cut in Test Room 4 of the WIPP facility (see map, Figure 1). These cores were cut with a Longyear 38 drill rig, using no liquid lubricant. The cores used in this study are designated RM-1 and RM-3; these were cut vertically upward into the roof, and directly opposite were cut vertically downward, respectively. The lithologic logs for these cores are shown in Appendix A.

Samples were chosen from approximately every other foot along the length of the cores. Brief descriptions of the portions selected, along with sample numbers and footages, are listed in Appendix B. Samples were selected from each of the dominant lithologies observed in the core. These are: (1) "clean" halite, (2) polyhalitic halite, (3) argillaceous halite, (4) mixed argillaceous-polyhalitic halite, and (5) anhydrites and clay seams. These samples, each ~ 6 in. long, were subsequently slabbed; one half was sent to Sandia for processing and analysis; the other remained in Carlsbad for the reference collection.

The technique used to process these samples has been described in detail (Stein, 1983). To summarize briefly, the samples, weighing from ~200 g to ~1 kg, were crushed to pieces the size of ≤ 1 cm^3. Weighed amounts of samples were then placed in large beakers of distilled water and stirred continuously until all salt was dissolved. The beakers were then decanted and the remaining residues were collected by filtration onto preweighed Whatman #3 filter papers, allowed to air-dry, and then weighed again. The dry weights of the water-insoluble residues are reported in Table 1. Small fractions of these residues were reserved for x-ray diffraction analysis; results are shown in Table 2. The

remaining portions were further processed by boiling for 4 hr (or longer, as necessary) in 0.25-M EDTA solution. This technique, developed by Bodine and Fernalld (1973), removes all divalent carbonates and sulfates from the water-insoluble residues. Following boiling, the samples were again collected onto preweighed Whatman #3 filter papers, dried, and weighed again to obtain the EDTA-insoluble residue weights (shown as weight percents) in Table 3. As before, where sample material was abundant enough, x-ray diffraction analyses were performed. These results are shown in Table 4.

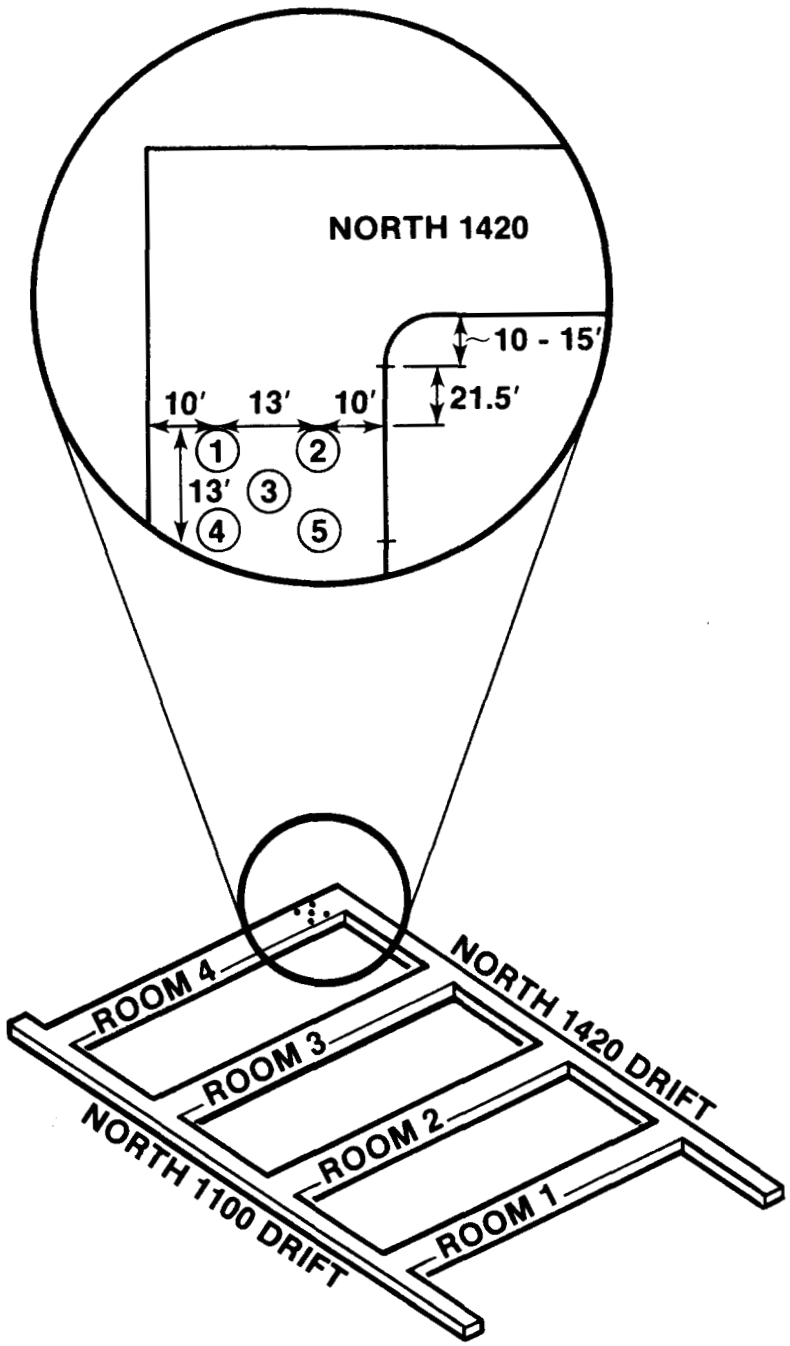

Figure 1. Map of underground workings (from Bechtel, 1985) showing location of Test Room 4 and location of core holes. (Note: Cores RM-3 and RM-4 are down; Cores RM-1 and RM-7 (not shown) are up.)

Table 1. Weight Percents of Water-Insoluble Residues

Sample No.	Sample Depth (ft) From	To	Sample Weight (g)	Weight of Water-Insoluble Residue (g)	Weight % (whole rock)
FH-201	2	2.5	757	2.76	0.36
FH-202	4	4.7	482	165.58	34.35
FH-203	8.3	9	649	13.09	2.02
FH-204	10.8	11.3	734	6.83	0.93
FH-205	13	13.55	715	0.38	0.05
FH-206	15.55	15.85	696	27.05	3.89
FH-207	16.9	17.45	700	1.41	0.2
FH-208	18.4	19.1	670.2	2.69	0.4
FH-209	19.65	20.05	641.3	1.1	0.17
FH-210	21.5	22	742.55	13.86	1.87
FH-211	23	23.5	700	3.6	0.51
FH-212	25.1	25.7	700	5.7	0.81
FH-213	26	26.5	700	4.57	0.65
FH-214	28.25	28.85	751	1.54	0.205
FH-215	30.5	31.05	700	0.47	0.07
FH-216	31	38	674	9.93	1.47
FH-217	39.25	39.85	535	13.42	2.51
FH-218	41	41.5	617.5	10.95	1.77
FH-219	42.5	43	676.5	21.13	3.12
FH-220	44	44.5	700	8.72	1.245
FH-221	45.3	45.85	743.85	4.04	0.54
FH-222	47	47.5	747.5	5.94	0.79
FH-223	49.05	49.55	739.5	2.2	0.3
FH-224	4	4.5**	385.6	235.74	61.14
*core loss zone					
**From RM-4					
FH-228	0.4	0.9	1,000	1.425	0.14
FH-229	2.3	2.8	1,000	0.77	0.08
FH-230	4.75	6.75	1,000	2.38	0.24
FH-231	7.1	7.3	600	169.89	28.32
FH-232	7.75	8.15	900	3.27	0.36
FH-233	8.15	9.1	1,000	0.45	0.05
FH-234	10.5	10.9	1,000	13.46	1.35
FH-235	12.5	12.6	1,000	2.87	0.29
FH-236	14	14.45	200	174.15	87.08
FH-237	16.1	16.6	700	12.99	1.86
FH-238	29	29.5	550	34.68	6.31
FH-239	34.05	34.5	600	18.58	3.1
FH-240	36.9	37.6	700	184.11	26.3
FH-241	38.2	38.7	1,000	3.04	0.3
FH-242	43.05	43.55	600	9.7	1.62
FH-243	47.2	47.7	850	6.41	0.75
FH-244	49.65	50	300	29.03	9.68
FH-245	51.3	52.1	400	37.19	9.3
FH-246*	20.05	20.45	1,000	8	0.8
FH-247*	23.45	23.95	600	81.2	13.53
FH-248*	25.5	26	1,000	0.47	0.05
FH-249*	45	45.65	900	4.96	0.55
*From RM-7					

Table 2. X-Ray Diffraction Results from Water-Insoluble Residues

Sample No.	Quartz (Q)	Magnesite (M)	Anhydrite (A)	Gypsum (G)	Halite (H)	Polyhalite (P)	Bassanite (B)	Approx. Abund.	Layer 14Å	Silicate 10Å	Basal 9.3Å	Plane Peaks 7Å
FH-201	+	+			+			Q>M>H				
FH-202		+?	+		+			A>H>M?				
FH-203	+	+	+					Q>A>M				
FH-204	+	+			Traces			M≥Q≥H				
FH-205	+											
FH-206	+	+	+		+			Q>A>M=H				
FH-207	+	+	+			+		M>Q>P≥A				
FH-208	+	+?	+	+	+			G>H≥A>Q>M				
FH-209	+	+						M>Q				
FH-210	+	+		+		+		P>G>M>Q				
FH-211	+	+	+		+			Q>M>H>A				
FH-212	+	+		+				M>Q>G				
FH-213	+	+						M≥Q				
FH-214				+		+		G>>P				
FH-215	Not enough sample available for x-ray diffraction study											
FH-216	+	+						M>Q				
FH-217	+	+		+				M>Q≥G				
FH-218	+	+			+			M>Q≥H				
FH-219	+	+						M≥Q				
FH-220	+	+						M>Q				
FH-221	+	+						M>Q				
FH-222	+	+						M>Q				
FH-223	+	+						M≥Q				
FH-224			+	+		+		A>G>P				
Note: These are x-ray diffraction results of bulk water-insoluble residues; no clay mineral fractions are reported here.												
FH-228	+	+							+	+		+
FH-229	+	Traces	+		Traces				+	+		+
FH-230	+	+							+	+		+
FH-231			+									
FH-232			+									
FH-233			+								+	
FH-234			+									
FH-235	+	+	+						+	+	+	+
FH-236			+									
FH-237			+	+	Traces		+					
FH-238	+	+							+	+		+
FH-239	+	+							+	+		+
FH-240	+	Traces	+	Traces								
FH-241			+									
FH-242	+	Traces	Traces						+	+		+
FH-243	+	Traces	+	Traces					+	+		+
FH-244	+	Traces	Traces						+	+		+
FH-245	+	+	Traces						+	+		+
FH-246	+	+	Traces						+	+		+
FH-247	Traces	Traces	+									
FH-248	+	Traces	+						+	+		+

Table 3. Weight Percents of EDTA-Insoluble Residues

Sample No.	Sample Depth (ft) From	To	Sample Weight (g)	Weight of EDTA-Insoluble Residue (g)	Weight % (water-insoluble residue)	Weight % (whole rock)
201	2	2.5	1.025	0.6	58.54	0.21
202	4	4.7	4	0.02	0.5	0.17
203	8.3	9	3	0.97	32.33	0.65
204	10.8	11.3	3	1.55	51.67	0.48
205	13	13.55	Insufficient material			
206	15.55	15.85	4	2.11	52.75	2.05
207	16.9	17.45	0.53	0.27	50.94	0.1
209	19.65	20.05	0.52	0.19	36.54	0.06
210	21.5	22	4	0.6	15	0.28
211	23	23.5	2.1	1.03	49.05	0.25
212	25.1	25.7	4	2.1	52.5	0.425
213	26	26.5	3.65	1.935	53.01	0.34
214	28.25	28.85	0.9	0.055	6.11	0.0125
215	30.5	31.05	Insufficient material			
216	31	38 *	4	2.43	60.75	0.89
217	39.25	39.85	4	1.5	37.5	0.94
218	41	41.5	4	1.95	48.75	0.86
219	42.5	43	4	2.27	56.75	1.77
220	44	44.5	4	2.61	65.25	0.81
221	45.3	45.85	2.3	1.48	64.35	0.35
222	47	47.5	4	2.3	57.5	0.45
223	49.05	49.55	1.075	0.46	42.79	0.13
224	4	4.5**	4	0.06	1.5	0.92
*Core loss zone						
**From RM-4						
228	0.4	0.9	0.7	0.255	36.4	0.05
229	2.3	2.8	0.475	0.15	31.6	0.025
230	4.75	6.75	2.075	0.955	46	0.11
231	7.1	7.3	4.1	0.005	0.12	0.03
232	7.75	8.15	3	0.21	7	0.025
233	8.15	9.1	0.38	0.09	23.7	0.01
234	10.5	10.9	3	0.005	0.17	0.002
235	12.15	12.6	2.5	0.65	26	0.001
236	14	14.45	3	0.007	0.23	0.2
237	16.1	16.6	3	0.16	5.3	0.1
238	29	29.5	2.9	1.29	44.5	2.81
239	34.05	34.5	3	1.315	43.8	1.36
240	36.9	37.6	3	0.07	2.3	0.6
241	38.2	38.7	2.8	0.02	0.71	0.002
242	43.05	43.55	3	2.03	67.7	1.1
243	47.2	47.7	3	0.86	28.7	0.215
244	49.65	50	3	1.76	58.7	5.68
245	51.3	52.1	2.7	0.645	23.9	2.22
246*	20.05	20.45	3	1.09	36.3	0.29
247*	23.45	23.95	3	0.08	2.67	0.36
248*	25.5	26	0.36	0.09	25	0.0125
249*	45	45.65	3	1.37	45.7	0.25

*From core RM-7

Table 4. X-Ray Diffraction Results from EDTA-Insoluble Residues

Sample No.	Quartz	Anhydrite	Magnesite	Polyhalite	Basal Planar Spacings 14 Å	10 Å
FH-201	+					
FH-202	Insufficient material					
FH-203	+					+
FH-204	+					
FH-205	Insufficient material					
FH-206	+					
FH-207	Insufficient material					
FH-208	+					
FH-209	Insufficient material					
FH-210	+	Traces		Traces		
FH-211	+				+	+
FH-212	+	Traces				
FH-213	+		Traces		+	+
FH-214	+					
FH-215	Insufficient material					
FH-216	+					
FH-217	+					+
FH-218	+					
FH-219	+				+	+
FH-220	+					
FH-221	+				+	+
FH-222	+				+	+
FH-223	+				+	+
FH-224	Insufficient material					

The components of the non-NaCl mineral residues were identified by x-ray diffraction. All x-ray analyses for this study were run by using a Phillips diffractometer with Cu Kα radiation at an operating voltage of 40 keV and 25 mA. The x-ray diffraction results obtained are at best only semiquantitative. Because of time constraints on the analyst and because of the limited amount of available sample material, it was decided to forego any attempts at more quantitative x-ray diffraction analysis at this time. Where indicated in Table 2, relative amounts of mineral species are reported on the bases of the analyst's inspection of the diffractograms and on his knowledge of the relative diffraction efficiencies of the different minerals present.

Some of the water- and EDTA-insoluble residue samples were observed to contain significant quantities of minute, well-developed, euhedral quartz crystals. A few of these crystals were hand-picked from selected water-insoluble residue samples by means of a binocular microscope and surgical tweezers. These crystals were then mounted on carbon bases and examined with a scanning electron microscope (SEM), as seen in Figure 2 (a-c). In addition to this quartz, very small ($\ll$10 μm) euhedral crystals of magnesite and Mg-silicate phases were also observed with the SEM and identified as to elemental content by EDAX.

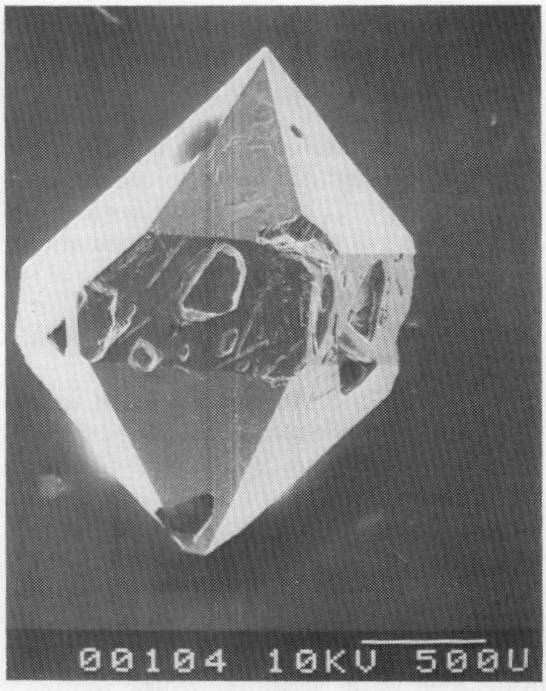

(a)

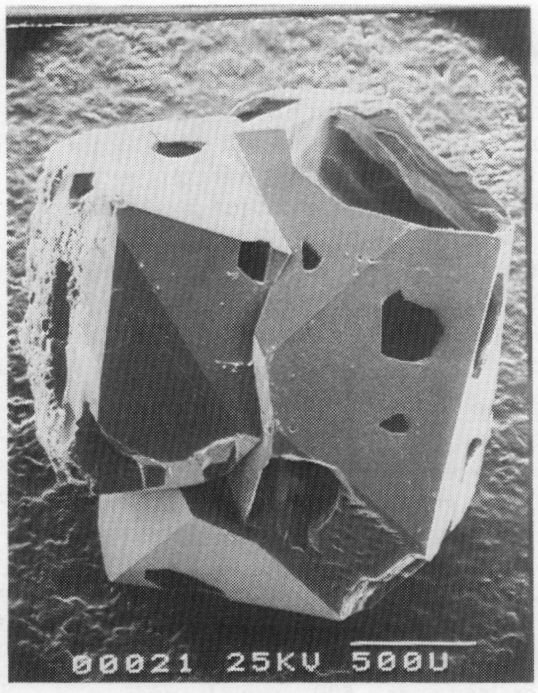

(b)

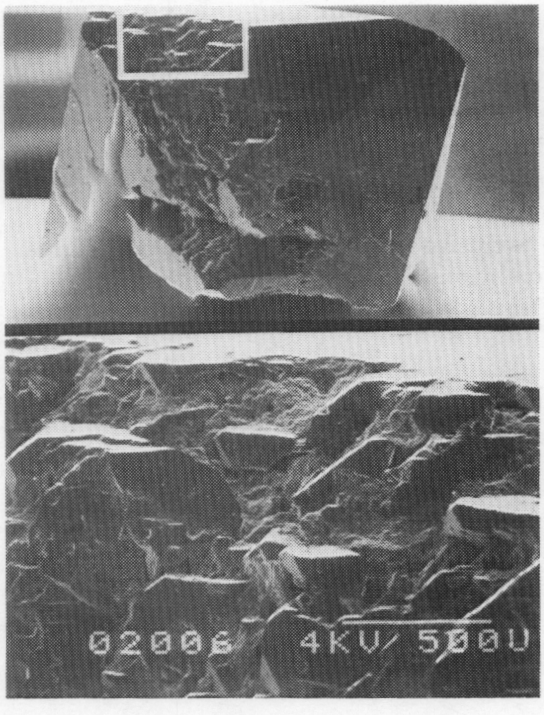

(c)

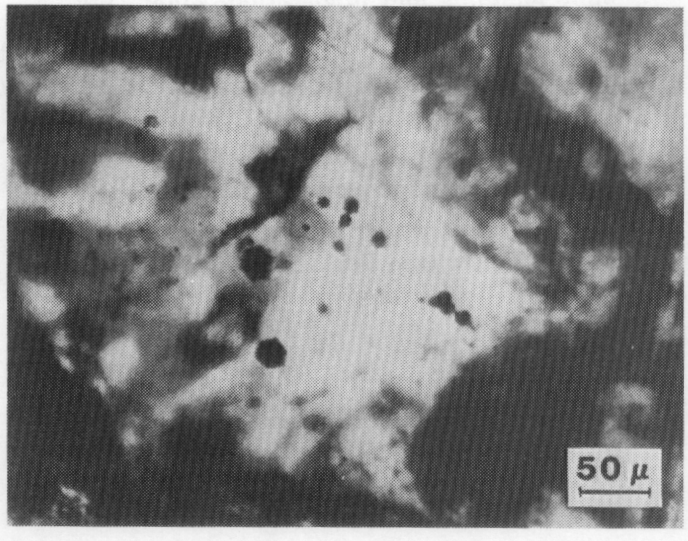

(d)

Figure 2. Scanning electron micrographs of authigenic quartz crystals found in water-insoluble residues from argillaceous halite ((a) – (c)) and thin section photomicrograph of authigenic quartz crystals in recrystallized halite (d).

The routine analytical procedure used in this study to determine weight percents of non-NaCl minerals, as described above, has two limitations: (1) it is time-consuming and labor-intensive; (2) this process yields weight percents of non-NaCl minerals as an average for a bulk sample; no information is obtained regarding the spatial distribution of these minerals within that sample. Therefore, two possible alternative techniques, gamma-beam densitometry and x-radiography, were selected on the basis of the following criteria:

- Rapid data acquisition: relative to the conventional analytical method described above, which requires weeks or months to process up to several meters of core, gamma-beam densitometry and x-radiography can analyze the same amount of core in hours or minutes, respectively.
- Continuous data collection: the information output is obtained from a continuous scan of the core, yielding far more data than integrating bulk mineralogy over a 500-g sample, while simultaneously showing the desired spatial distribution of non-NaCl components.
- Sample handling and preparation: whole core was used for x-radiography, and only surface milling in a lathe was required for the gamma beam densitometer. Because both of these techniques are nondestructive, the information thus obtained may then be supplemented by thin sections or other mineralogical analyses.

A "trial" halite core (actually, a scrap core of unspecified location within the facility horizon) was selected on the basis of the apparent presence of large and variable amounts of clays and other mineral impurities as ascertained by visual inspection. This core was first subjected to scanning by a gamma-beam attenuation system accountable to Sandia's Department 1510. For further details of this procedure, see Reda and Hadley (1983). This technique uses a Cs^{137} source to produce a photon beam. The attenuation coefficient, μ, of this beam through the core material is compared to the measured value for a reference sample of pure salt (μ_{ref}). The results of the gamma-beam densitometer scan are shown in Figure 3(a).

The same piece of core was also subjected to x-radiography and the film then read by microdensitometry; results are shown in Figure 3(b). A large fracture in the core, which showed up on the x-radiograph as a dark line, is offset from the position of the same fracture on the gamma-beam densitometer plot (Figures 3(a) and 3(b)) as a result of the slight rotation of the core from its position in the x-radiographs.

Finally, the core was sliced into ~1-in. pieces and dissolved in distilled water according to the routine procedure. The total dry weight percent of mineral residue is plotted in Figure 3(b) and represents an average value over every 1-in. length of core.

Gamma-beam densitometry appears to be the least suitable of these techniques for detecting mineral impurities in halite core. No obvious correlation exists between the data in Figure 3(a) and in Figure 3(c). The x-radiograph results, however, may be fit by a smooth curve that reasonably approximates the conventional analytical data (Figures 3(b) and 3(c), respectively) exclusive of such features as peaks corresponding to obvious fractures.

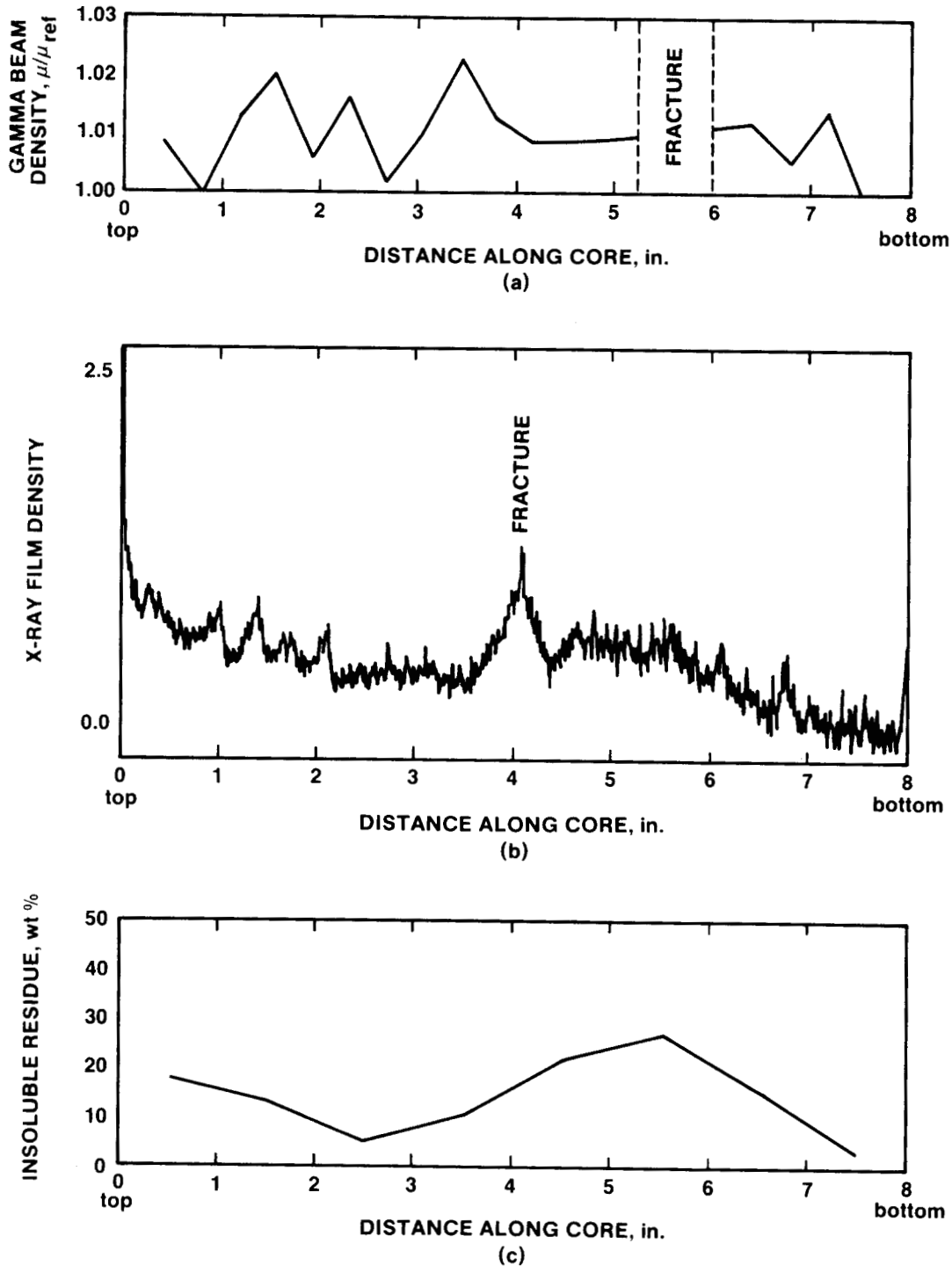

Figure 3. Comparison of three different methods of detection of non-NaCl mineralogy by using surplus core from the WIPP facility horizon: (a) gamma-beam densitometry, (b) x-radiography, and (c) conventional dissolution technique.

Discussion

The primary purpose of this study was to examine closely the non-NaCl constituents of halite in the lower Salado Formation as a means of characterizing the lithology of the WIPP host rock in terms of abundance, distribution, and identification of trace mineral components.

By way of addressing the first of these, the data presented in Tables 1 and 3 are consistent with similar analyses performed for the SPDV program. For the samples analyzed in the study reported here, weight percents of water-insoluble residues ranged from 0.05 to 87.08 wt%. For the EDTA-insoluble residues, weight percents ranged from 0.001 to 5.68 wt% of the total weights. The mean values for the water- and EDTA-insoluble residues are 5.56 wt% and 0.64 wt%, respectively. The occasional excursions from the average numbers were attributed to unusually clay-rich layers or seams and/or to distinct anhydrite units. Linear statistics for these data are found in Table 5.

One of the most significant conclusions gained from the SPDV work is that the measurements of the non-NaCl mineralogy, as weight percents, are smaller by at least an order of magnitude than previous estimates made by visual observations. Many of the WIPP lithologic logs that predate the SPDV mineralogy study report the presence of polyhalite and clays in amounts ranging from 30 to 50 wt% or more. The SPDV results show that only a very small amount of non-NaCl material can impart such color and opacity to the salt so as to create the visual impression of a much larger quantity. For this reason, it was decided to put portions of the samples used in this study together with the data from the water- and EDTA-insoluble residue analyses into a reference collection in order to better "calibrate" visual estimates and therefore enable visual core descriptions to be made more quantitatively.

It is much more difficult, however, to describe and quantify the distribution of non-NaCl minerals dispersed in a halite core. For example, consider a halite sample weighing 500 g and containing 5% clay by weight. The analytical techniques used in this study (the results of which are shown in Tables 1 and 3) do not distinguish the distribution of this amount of clay in this particular sample interval. It could be present as fine particles evenly disseminated throughout the halite; it may occur as intergranular in-fillings or as large blebs; it may be present as a single discrete layer or seam in otherwise "clean" halite; or it may be some combination of all of these. While clay seams or layers are, for the most part, visually conspicuous enough to be noted as such in the lithologic logs, the distribution of trace minerals in most halitic core is obscure enough that an accurate characterization would best be obtained by detailed examination of many thin sections. This approach is out of the question, given the volume of core required for this study and time constraints on the analyst. An attempt was therefore made to develop a technique that would be both rapid and nondestructive, yielding an accurate determination of the distribution of trace minerals and at the same time preserving the core intact for future use. Variations in gamma-beam densitometry as a function of mineralogy are slight. Measurements of film density of the x-radiographs appear to be significantly more sensitive and to parallel the results of the mineralogical determinations made by using the conventional technique described in this report.

As shown in Table 2, the water-insoluble mineralogy of these samples consists of quartz, magnesite, anhydrite, gypsum, polyhalite, alkali feldspar, and clays. Because of the complexity of the analytical process required to distinguish clay mineral species (separation of the clay fraction, heat treatment, exposure to ethylene glycol, etc), we report here only the basal planar spacings observed in the diffractograms of these samples. Major peaks belonging to clay minerals were observed at 14 Å, 10 Å, 9.3 Å, and 7 Å. Detailed clay mineralogical analyses on these and other WIPP samples are in progress; results will be presented in a later report. The EDTA-insoluble mineralogy (Table 4) consists entirely of quartz and clays except for a few samples showing traces of anhydrite, magnesite, and polyhalite, where EDTA digestion was obviously incomplete. Again, as described in the preceding paragraph, the clay minerals have not been identified as particular individual species, but only by the presence or absence of major peaks.

Most of the quartz (>90%, based on binocular microscope inspection of the samples in which it was found) appears to consist of well-developed, doubly terminated euhedral crystals. This morphology is highly suggestive of an authigenic origin. First observed in the SPDV samples, these quartz crystals appear to be associated exclusively with clay-bearing or "argillaceous" halite, as described in the lithologic logs. This association implies an origin of authigenic quartz through diagenetic alteration of the clay minerals; one possible mechanism is (from Siever, 1962):

$$\text{montmorillonite} \longrightarrow \text{illite} + SiO_2$$

The authigenic morphologies (Figures 2(a) – (c)) together with the textural relationships as seen in thin section (Figure 2(d)) also suggest that clay diagenesis and quartz precipitation preceded halite recrystallization.

Table 5. Statistics on Weight-Percent Data

Water-Insoluble Residues		EDTA-Insoluble Residues	
M	0.45000D+02	M	0.42000D+02
Mean	0.55620D+01	Mean	0.63524D+00
Std. Dev.	0.14567D+02	Std. Dev.	0.10344D+01
Variance	0.21218D+03	Variance	0.10701D+01
Max. X	0.87080D+02	Max. X	0.56600D+01
Min. X	0.50000D−01	Min. X	0.10000D−02
Range	0.07030D+02	Range	0.56790D+01
Sum. X	0.25029D+03	Sum. X	0.26680D+02
Sum. X Square	0.10728D+05	Sum. X Square	0.60821D+02
Correction Term	0.13921D+04	Correction Term	0.16948D+02
Sum. Small X Square	0.93361D+04	Sum. Small X Square	0.43873D+02
Std. Dev. (Mean)	0.21715D+01	Std. Dev. (Mean)	0.15962D+00
Variance (Mean)	0.47152D+01	Variance (Mean)	0.25478D−01
Normality Test		Normality Test	
Mean Dev.	0.75722D+01	Mean Dev.	0.64367D+00
Third Moment	0.12952D+05	Third Moment	0.34221D+01
Fourth Moment	0.10072D+07	Fourth Moment	0.16297D+02
A	0.52571D+00	A	0.62978D+00
Sort B Sub1	0.43342D+01	Sort B Sub1	0.32053D+01
B Sub2	0.23399D+02	B Sub2	0.14935D+02
D-Test Statistic	0.98294D+01	D-Test Statistic	0.49859D+01

A simple mass balance calculation (Stein, 1984) clearly indicates that the volume of authigenic quartz present in these halite samples is, on the average, greater by almost two orders of magnitude than that which could have been produced by simple evaporation of seawater alone. Further studies of authigenic silicate formation and clay diagenesis are in progress. In addition to the quartz, other authigenic minerals may be present; authigenic feldspars and pyrite and possibly a zeolite have been identified by the author in thin-section, x-ray diffraction, and SEM work on some of the samples in this study. Because these results are preliminary, further details are not included here but will be reported on at a later date.

Figures 4 and 5 illustrate the relationship between weight percents of water- and EDTA-insoluble residues and lithology, as seen in the cores from which these samples were taken. No obvious correlation exists between the non-NaCl mineralogy and distance from the repository in either the up or down direction. However, these figures indicate that samples from anhydrite-bearing units contain the largest amounts of insoluble residues. Perhaps not surprisingly, samples from the visually designated "clean" halites contain the least. Moreover, in Figures 4 and 5, two lines are used for each sample interval to represent weight percents of water- and EDTA-insoluble residues. The larger the difference between these two lines in any one sample, the greater the relative abundance of the EDTA-soluble component (mainly the sulfate minerals polyhalite and anhydrite). This is clearly seen in samples such as FH-231, FH-236, and FH-240, taken from distinct anhydrite units in core RM-1 at depths of 7.1 to 7.3 ft, 14 to 14.45 ft, and 36.9 to 37.6 ft, respectively. Conversely, where the difference between each pair of lines is small (for example, FH-239, FH-242, or FH-217 through FH-224), the amounts of water- and EDTA-insoluble residues are nearly equal and thus composed primarily of insoluble silicate residues (quartz and clays) as is typically seen in the zones of argillaceous halite.

It is beyond the scope of this report to discuss the effects of trace mineralogy in WIPP salt on material properties or on creep behavior in rock salt. It is intended that the data reported here will be used to further modify the structural computations as discussed in Krieg et al (1980). This report is intended for use as a supplement to Krieg et al (1982) and Krieg (1984), by providing a more complete reference stratigraphy that includes detailed analyses of the halite mineralogy.

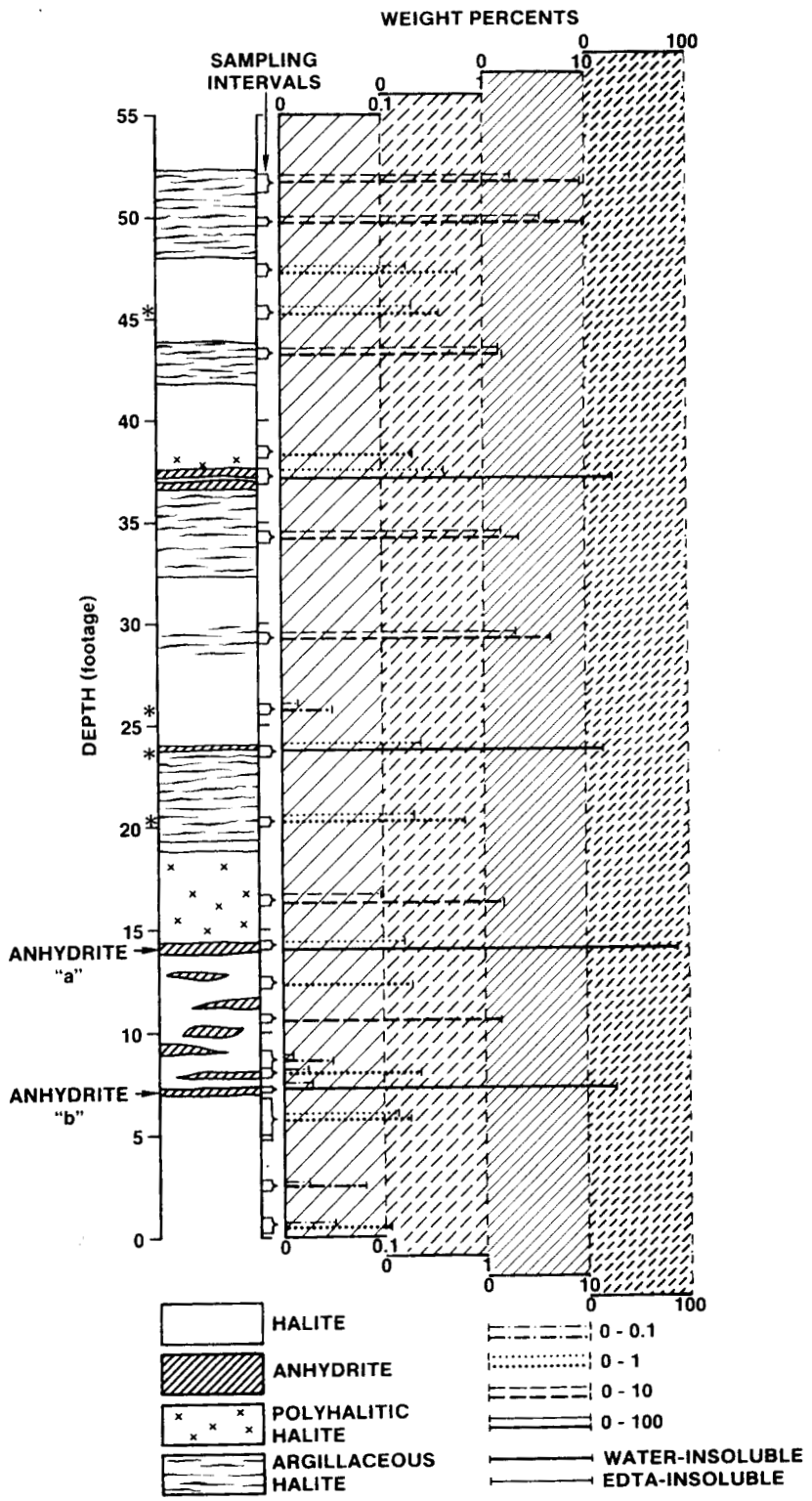

Figure 4. Core RM-1, showing lithologies and amounts of water- and EDTA-insoluble residues. (RM-7 samples are from another core, taken in the up direction, in close proximity to RM-1 (see Figure 1).)

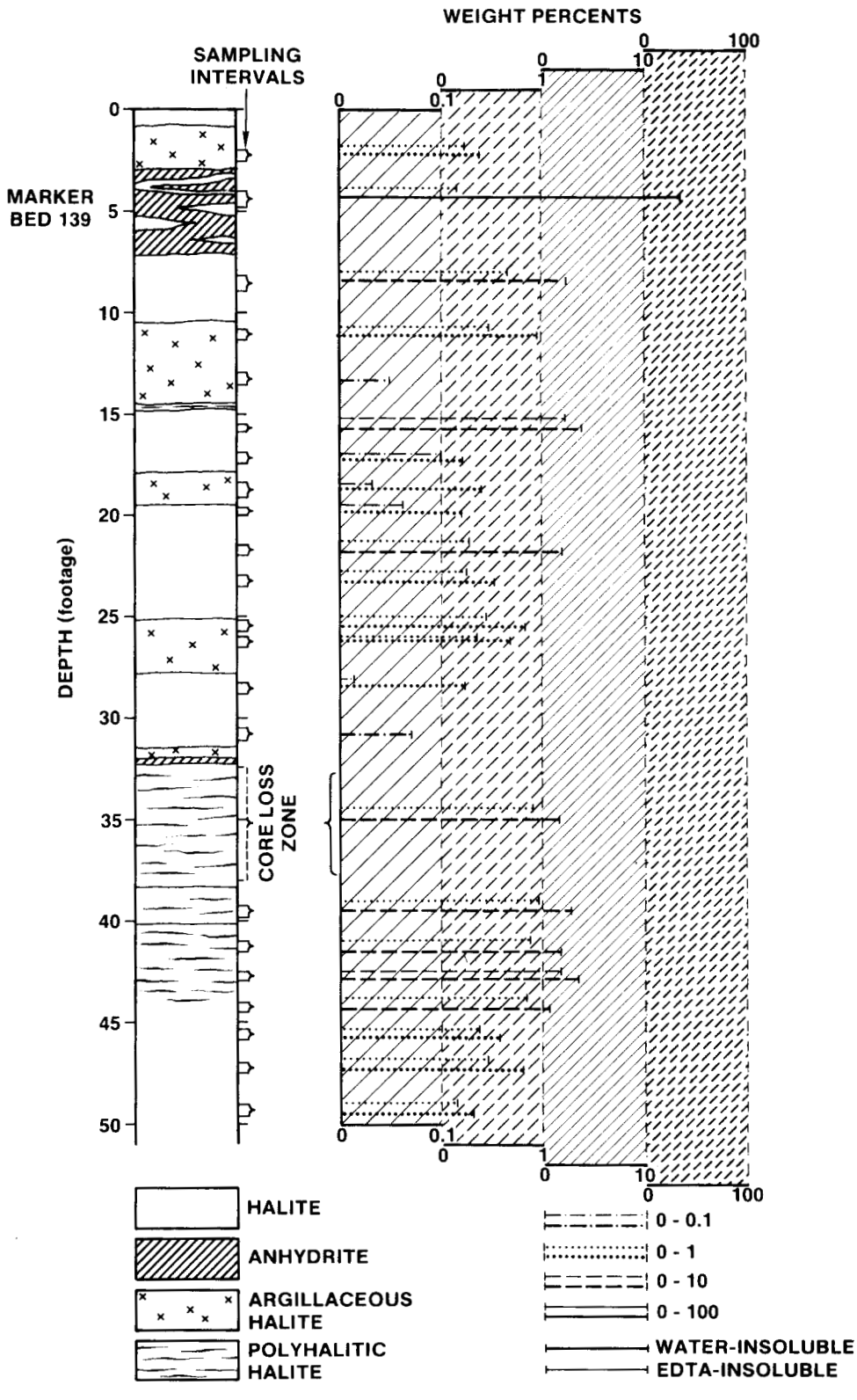

Figure 5. Core RM-3, showing lithologies and amounts of water- and EDTA-insoluble residues.

Conclusions

In summary, we report here the quantities, distribution, and mineralogical species of the non-NaCl components of halite and anydrites in the immediate vicinity (e.g., within 100 vertical feet) of the WIPP facility horizon. These components, as determined by x-ray diffraction, consist of quartz, anhydrite, gypsum, magnesite, polyhalite, and clays, with traces of alkali feldspar and possible zeolites. The quartz is primarily authigenic and is probably derived from alteration of the clay minerals. Textural relations indicate that this alteration and precipitation of the authigentic quartz either preceded or perhaps occurred simultaneously with halite recrystallization.

The results of the analyses presented herein confirm previous conclusions regarding discrepancies between visual estimates of mineral impurities in WIPP core and accurate measurements, as obtained by the precedure defined during the SPDV investigation. It has been shown that visual estimates of trace minerals may be too high by as much as an order of magnitude. WIPP salt contains, on the average, <5 wt% mineral impurities, except in areas of well-defined anhydrite or clay bands or layers. These impurities occur as either finely divided particles dispersed throughout the halite, as intergranular coatings, or as discrete blebs, lenses, laminae, or seams.

The analytical procedure used to produce the results reported here is time-consuming and provides no detailed information as to the distribution of non-NaCl minerals. Alternative methods of sample analysis are being investigated. It appears that x-radiography of halite core is rapid, nondestructive, and accurately reflects mineral impurities in the salt. More work is necessary before this technique can be considered a quantitative tool for this type of examination. However, the data obtained from the samples analyzed in this study will be used as points for calibration.

References

M. W. Bodine, Jr., and T. H. Fernalld, "EDTA Dissolution of Gypsum, Anhydrite, and Ca-Mg Carbonates," *J Sed Petrology* 43:4, 1152-1156 (1973).

Bechtel National, Inc., for US Dept. of Energy, *Quarterly Geotechnical Field Data Report*, Section B.O: Test Rooms; WIPP-DOE-199 (May 1985).

R. D. Krieg, H. S. Morgan, and T. O. Hunter, *Second Benchmark Problem for WIPP Structural Computations*, SAND80-1331 (Albuquerque, NM: Sandia National Laboratories, December 1980).

Memo, R. D. Krieg, D. Powers, and R. Price of Sandia National Laboratories (SNL), to D. E. Munson of SNL, "Proposed September '82 WIPP stratigraphy," September 20, 1982.

R. D. Krieg, *Reference Stratigraphy and Rock Properties for the Waste Isolation Pilot Plant (WIPP) Project*, SAND83-1908 (Albuquerque, NM: Sandia National Laboratories, January 1984).

Memo, D. C. Reda and G. R. Hadley of SNL to C. L. Stein of SNL, "Salt Core Characterization Via Gamma-Beam Attenuation Measurements," September 9, 1983.

R. Siever, "Silica Solubility, 0° – 200°C, and the Diagenesis of Siliceous Sediments," *J Geol 70*, pp 127-150 (1962).

C. L. Stein, Supporting Document 11: "Mineralogical Content of Interval Strata"; Supporting Document 12: "Location and Characterization of Interbedded Materials," in *Results of Site Validation Experiments*, vol. 2, Supporting Document 5-14. Waste Isolation Pilot Plant, TME 3177 (1983).

C. L. Stein, "Authigenic Quartz in Halite from the Delaware Basin., Southeastern New Mexico (submitted to *J Geol*, August 1984).

Appendix A

Lithologic Logs

Core: RM-1
Direction of drilling: Vertical up
Location: Test Room 4 (roof)
Mine Coordinates: N1364 W631 approx.
Depth of Borehole: 52.1 ft
Logged by: J. E. Gallerani

Elev. above Ceiling (ft)		
From	To	
0	7.05	*Halite*: clear to medium reddish-orange to light gray, coarsely crystalline, hard. Fine to medium crystalline at 6 to 7.05 ft. Trace (<1/2%) polyhalite. Trace (<1%) gray clay.
7.05	7.2	*Anhydrite (anhydrite "b")*: very light gray to medium gray, microcrystalline; hard. Some patches of halite within. Trace gray clay at 7.05 ft. Irregular upper surface at 7.2 ft.
7.2	13.9	*Halite*: clear to medium reddish-orange, medium to coarsely crystalline, hard. White anhydrite stringers and laminae found within core. Beginning at 12.3 ft trace gray clay (<1%). Core medium grading to fine-medium crystalline toward anhydrite.
13.9	14.4	*Anhydrite*: very light gray to medium gray, microcrystalline, hard. Scattered halite. Trace gray clay at 13.9 ft. Upper contact at 14.4 ft is irregular, tightly welded.
14.44	18.8	*Polyhalitic halite*: clear to medium reddish-brown-orange, coarsely crystalline, moderately hard to hard. Contains blebs and patches of polyhalite (1% to 5%), locally >5%.
18.8	19.3	*Halite*: clear, coarsely crystalline, hard. Scattered polyhalite blebs (<1%).
19.3	24.05	*Argillaceous halite*: clear to medium grayish-brown, fine to coarsely crystalline, medium hard to hard. Contains gray and brown clay, generally <2%. Trace medium reddish-orange color. Gray anhydrite layer at 23.85 to 24 ft, thin gray lamina immediately beneath.
24.05	32.4	*Halite*: clear, coarsely crystalline, hard. Several irregular white patches at 25 to 25.7 ft. Clear to medium brown from 28.3 to 29.5 ft; brown clay (1% to 2%) breaks at 29 ft and 29.25 ft.
32.4	36.65	*Argillaceous halite*: clear to medium reddish-brown and grayish-brown, coarsely crystalline, medium hard to hard. Dispersed argillaceous, predominantly brown. Avg. <1% to 3%, locally >5%.
36.65	37.6	*Anhydrite*: very light gray to medium gray, microcrystalline hard anhydrite with irregular zone of halite at ~37.15 to 37.35 ft. Upper contact irregular, tightly welded. Gray clay at 36.7 ft.

Elev. above Ceiling (ft) From	To	
37.6	41.8	*Halite*: clear to medium reddish-orange, coarsely crystalline, hard. Contains <1% polyhalite (dispersed reddish-orange color). Core contains highest % polyhalite 37.6 to 38.2 ft, scattered white (magnesite) stringers.
41.8	43.9	*Argillaceous halite*: clear to medium brown, coarsely crystalline with some fine, medium hard to hard. Predominantly brown argillaceous 1% to 3%, locally up to 5%.
43.9	48	*Halite*: clear to medium brown, fine to coarsely crystalline, medium hard. Trace (<1%) argillaceous and polyhalite.
48	52.1	*Argillaceous halite*: clear to medium brown, medium with some fine to coarsely crystalline, medium hard to hard. Brown argillaceous (1% to 5%, avg. 1% to 2%. Clay break at 52.1 ft. 5% to >10% brown clay at 49.6 to 50.2 ft. Trace (<1%) polyhalite.

Core: RM-4
Direction of drilling: Vertical down
Location: Test Room 4 (floor)
Mine Coordinates: N1362.6 W627.5
Depth of Borehole: 49.5 ft
Logged by: J. E. Gallerani

Depth below floor (ft) From	To	
0	2.7	*Halite*: clear to medium brown, medium to coarsely crystalline, medium hard to hard. Trace (<1%) polyhalite and gray clay.
2.7	6.85	*Anhydrite (MB-139)*: mixture of medium reddish-orange polyhalite, polyhalitic halite and anhydrite from 2.7 to 4.2 ft. Coarsely crystalline polyhalitic halite mixed with polyhalitic and microcrystalline anhydrite, approx. 40% to 60%. Grades to higher % anhydrite 4.2 to 5.6 ft. From 5.6 to 6.85 ft is anhydrite. Very light gray to white microcrystalline, laminated anhydrite mixed with 10% to 30% polyhalite and polyhalitic halite, hard. Core broken in small pieces at 4.4 to 4.6 ft. Trace gray clay at 6.85 ft.
6.85	10.3	*Halite*: clear to grayish to medium reddish-orange, medium to coarsely crystalline, hard. Gray clay <1%, scattered clay breaks. Trace (<1%) polyhalite.
10.3	14.1	*Polyhalitic halite*: clear to medium reddish-orange, coarsely crystalline, hard. Polyhalite <1% to 3%, locally >3%. Scattered gray clay breaks to 11.3 ft.
14.1	16.6	*Halite*: clear to light-gray to medium reddish-orange, medium to coarsely crystalline, hard. Trace (<1%) gray clay. Parting at 14.3 ft. Scattered clay breaks, <1% polyhalitic.
16.6	17.7	*Halite*: clear with trace of medium reddish-orange, coarsely crystalline, hard. Trace (<1%) polyhalite.
17.7	19.9	*Halite*: clear to medium reddish-orange-brown, coarsely crystalline, hard. Generally <1% polyhalite with local zones to 3%. From 18.4 to 19.6 ft, up to 5% polyhalite.
19.9	26.5	*Halite*: clear mottled with medium reddish-orange and light gray, medium to coarsely crystalline, hard. Gray clay <1%. <1% polyhalite with local zones to 2%.

Depth below floor (ft)		
From	To	
26.5	32.05	*Halite*: clear to medium reddish-orange-brown, coarsely crystalline, hard, polyhalitic. Up to 5% polyhalite from ~26.5 to 27.5 ft decreasing to avg <1% polyhalite below 29.5 ft. Mostly anhydrite at 31.45 to 31.65 ft. Clear halite 30.65 to 31.45 ft.
32.4	39.5	*Halite*: clear to medium reddish-orange and medium-dark gray, medium to coarsely crystalline, hard. Trace (<1%) gray clay and trace (<1%) scattered polyhalite blebs. Core broken up in very small pieces (gravel-size up to 1 in.) at 33.4 to 33.75 ft.
39.5	43	*Halite*: clear to medium brown, medium to coarsely crystalline, medium hard to hard. Contains <1% to 3% predominantly brown argillaceous, clay breaks scattered within. Trace (<1/2%) polyhalite dispersed throughout.
43	50.2	*Halite*: clear mottled with traces (<1%) of gray clay and medium reddish-orange polyhalite blebs. Medium to coarsely crystalline, hard. Up to 3% gray argillaceous at 48.55 to 49.1 ft.

Core: RM-3
Direction of drilling: Vertical down
Location: Test Room 4 (floor)
Mine Coordinates: N1361 W631 approx.
Depth of Borehole: 51.05 ft
Logged by: J. E. Gallerani

Depth below floor (ft)		
From	To	
0	0.9	*Halite*: clear, coarsely crystalline, hard. Trace (<1/2%) polyhalite blebs and gray clay.
0.9	3	*Polyhalitic halite*: clear to medium reddish-orange, coarsely crystalline hard. <1% polyhalite increasing to ~3% to 4% toward lower part of section.
3	7.2	*Anhydrite (MB-139)*: mixture of 50/50% anhydrite and halite from 3 to 3.9 ft. Upper contact is irregular at 20° to 25° dip. Core hard. From 3.9 to 7.2 ft, very light to medium gray, microcrystalline, hard. Contains halite and polyhalitic halite within. Core loss most probably in this zone.
7.2	10.45	*Halite*: clear to light gray, medium to coarsely crystalline, medium hard to hard. Gray argillaceous <1%.
10.45	14.8	*Polyhalitic halite*: clear to medium reddish-orange, coarsely crystalline, hard. Trace <1/2% gray clay, <1% to 3% polyhalite. 3/4 in. irregular polyhalite layer at 14.6 ft. Dark gray clay seam up to 3/4 in. at ~14.8 ft.
14.8	16.5	*Halite*: clear to light gray, fine to coarsely crystalline, medium hard to hard. Trace (<1%) polyhalite and gray clay.
16.5	17.9	*Halite*: clear with some medium reddish-orange, coarsely crystalline, hard. <1% polyhalite.
17.9	19.5	*Polyhalitic halite*: clear to medium reddish-orange-brown, coarsely crystalline, hard. <1% to 5% polyhalite, trace (<1/2%) gray clay.
19.5	32	*Halite*: clear, mottled with medium reddish-orange, fine to coarsely crystalline, medium hard to hard. Trace (<1% to 2%) gray clay and <1% to 2% polyhalite with local zones >3%. Clay breaks scattered within core. Polyhalitic halite at 25.2 to 27.8 ft. Avg 2% to 4% polyhalite. No clay at 27.8 to 30.1 ft. >10% polyhalite at 31.55 to 31.75 ft.

Depth below floor (ft)		
From	To	
32.0	32.1	*Anhydrite*: very light gray to light-gray anhydrite mixed with some halite. Microcrystalline, hard. Trace gray clay at 32.1 ft. Core loss from 30.75 to 35.75 ft. Depth of anhydrite based on boring RM-2.
32.1	38.3	*Halite*: clear with some medium reddish-orange and light gray. Medium to coarsely crystalline, medium hard to hard. Trace (<1%) gray clay and polyhalite. Core loss in this section.
38.3	51.05	*Halite*: clear to light gray mottled with medium reddish-orange polyhalite. Coarsely crystalline, hard. Avg <1% to 4% gray clay. Clay breaks irregular and low angle, commonly scattered in core to ~44 ft. <1% clay from 44 ft to bottom of hole. <1% polyhalite average with 1% to 2% polyhalite 38.3 to 40.15 ft.

Appendix B

Description of Core Samples Used In This Study

Split Core Samples for Geochemistry Analysis

Sample No.	Hole No.	Depth Interval (ft)		Sample Description
		From	To	
FH-201	RM-3	2	2.5	Clear with trace polyhalite
FH-202	RM-3	4	4.7	Polyhalitic halite
FH-203	RM-3	8.3	9	8.3 to 8.5 ft – mixed clay/polyhalite 8.5 to 9 ft – clear
FH-204	RM-3	10.8	11.3	Clear, trace polyhalite (5 pieces)
FH-205	RM-3	13	13.55	Polyhalitic (4 pieces)
FH-206	RM-3	15.55	15.85	Mixed clay/polyhalite
FH-207	RM-3	16.9	17.45	Clear, coarsely crystalline, trace polyhalite
FH-208	RM-3	18.4	19.1	Polyhalitic (3 pieces)
FH-209	RM-3	19.65	20.05	Polyhalitic (3 pieces)
FH-210	RM-3	21.5	22	Clear mottled with polyhalite
FH-211	RM-3	23	23.5	Same as above
FH-212	RM-3	25.1	25.7	Clear to mod. reddish-orange, trace polyhalite
FH-213	RM-3	26	26.5	Clear to mod. reddish-orange, trace polyhalite
FH-214	RM-3	28.25	28.85	Same as above with some horizontal fractures
FH-215	RM-3	30.5	31.05	Clear, coarsely crystalline, very little polyhalite
FH-216	RM-3	31	38	Clear, trace gray clay, polyhalite
		(Core loss zone)		
FH-217	RM-3	39.25	39.85	Grayish-brown mixed clay/polyhalite
FH-218	RM-3	41	41.5	Mixed clay/polyhalite, coarsely crystalline, very little polyhalite
FH-219	RM-3	42.5	43	Mixed clay/polyhalite, medium coarsely crystalline, very little polyhalite
FH-220	RM-3	44	44.5	Mixed clay/polyhalite, coarsely crystalline
FH-221	RM-3	45.3	45.85	Clear, coarsely crystalline
FH-222	RM-3	47	47.5	Clear, trace gray clay
FH-223	RM-3	49.05	49.55	Clear, trace gray clay/polyhalite
FH-224	RM-3	4	4.5	Medium reddish-orange polyhalite/anhydrite
Core Samples for Geomechanical Testing				
FH-225	RM-4	40.75	42.5	Mixed clay/polyhalite
FH-226	RM-4	42.5	44	Mixed clay/polyhalite
FH-227	RM-5	39.05	41.6	Mixed clay/polyhalite
FH-228	RM-1	0.4	0.9	Halite, clear to medium reddish-brown to light gray, coarsely, some fine to medium crystalline. Trace polyhalite and clay
FH-229	RM-1	2.3	2.8	Same as above
FH-230	RM-1	4.75	6.75	Same as above
FH-231	RM-1	7.1	7.3	Anhydrite "b" with halite 7.2 to 7.3 ft

Sample No.	Hole No.	Depth Interval (ft)		Sample Description
		From	To	
FH-232	RM-1	7.75	8.15	Halite, clear to medium reddish-orange, medium to coarsely crystalline, white anhydrite stringers
FH-233	RM-1	8.15	9.1	Same as above
FH-234	RM-1	10.5	10.9	Same as above
FH-235	RM-1	12.15	12.6	Same with trace gray clay
FH-236	RM-1	14	14.45	Anhydrite "a"
FH-237	RM-1	16.1	16.6	Polyhalite halite
FH-238	RM-1	29	29.5	Halite with brown clay, coarsely crystalline
FH-239	RM-1	34.05	34.5	Argillaceous halite
FH-240	RM-1	36.9	37.6	Anhydrite with some halite
FH-241	RM-1	38.2	38.7	Halite with trace polyhalite, magnesite stringers
FH-242	RM-1	43.05	43.55	Argillaceous halite
FH-243	RM-1	47.2	47.7	Halite, trace polyhalite and clay
FH-244	RM-1	49.65	50	Argillaceous halite
FH-245	RM-1	51.3	52.1	Argillaceous halite, break at 52.1 ft
FH-246	RM-7	20.05	20.45	Halite, trace of clay and polyhalite
FH-247	RM-7	23.45	23.95	Halite with gray anhydrite, trace clay
FH-248	RM-7	25.5	26	Halite – clear, coarsely crystalline
FH-249	RM-7	45	45.65	Halite, trace brown clay, coarsely crystalline

DISTRIBUTION:

US Department of Energy, Headquarters (2)
Office of Nuclear Waste Management
Attn: A. Follett, Project Coordinator (WIPP)
R. Stein
Washington, DC 20545

US Department of Energy (2)
Albuquerque Operations Office
Attn: G. C. Romatowski
D. G. Jackson, Dir, Public Affairs Div
PO Box 5400
Albuquerque, NM 87185

US Department of Energy (6)
Attn: W. R. Cooper
Carlsbad WIPP Project Office (2)
A. Hunt, WPO (Carlsbad) (4)
PO Box 3090
Carlsbad, NM 88221

US Department of Energy
Carlsbad WIPP Project Office
Room 113, Federal Bldg
Carlsbad, NM 88220

US Department of Energy, NPO (2)
Office of Nuclear Waste Isolation
Attn: Jeff O. Neff
R. Wunderlich
505 King Ave
Columbus, OH 43201

US Department of Energy
Richland Operations Office
Nuclear Fuel Cycle and Production Div
Attn: R. E. Gerton
PO Box 500
Richland, WA 99352

US Department of Energy
Research and Tech Support Div
Attn: D .E. Large
PO Box E
Oak Ridge, TN 37830

US Department of Energy (2)
Division of Waste Products
Attn: G. H. Daly
J. E. Dieckhoner
Mail Stop B-107
Washington, DC 20545

US Department of Energy (2)
Idaho Operations Office
Nuclear Fuel Cycle Div
Attn: R. M. Nelson
J. Whitsett
550 Second St
Idaho Falls, ID 83401

US Department of Energy (4)
Savannah River Operations Office
Waste Management Project Office
Attn: J. R. Covell
D. Fulmer
S. Cowan
W. J. Brumley
PO Box A
Aiken, SC 29801

US Nuclear Regulatory Commission (3)
Division of Waste Management
Attn: Michael Bell
Hubart Miller
Jacob Philip
Mail Stop 697SS
Washington, DC 20555

US Nuclear Regulatory Commission
HLW Licensing Branch, Materials Section
Attn: F. R. Cook
MS 905 SS
Washington, DC 20555

Battelle Memorial Inst (17)
Project Management Div
Attn: W. Carbiener, General Manager (3)
S. Basham
D. E. Clark
S. Goldsmith
J. E. Hanley
P. Hoffman
H. R. Hume
H. N. Kalia
J. Kircher
S. Matthews
D. Moak
J. Moody
G. Raines
J. Treadwell
ONWI Library
505 King Ave
Columbus, OH 43201

DISTRIBUTION (cont):

Battelle Pacific Northwest Labs (4)
Attn: D. J. Bradley
J. Relyea
R. P. Turcotte
R. E. Westerman
Battelle Blvd
Richland, WA 99352

Westinghouse Electric Corp (9)
Attn: P. Miskimin
V. Likar
L. Cole
V. DeJong
R. Gehrman
J. Johnson
J. W. Sadler
J. E. Stumbaugh
Library
PO Box 2078
Carlsbad, NM 88221

Bechtel, Inc (5)
Attn: E. Weber
H. Taylor
P. Frobenius
D. L. Wu
W. T. Li
45-11-B34
PO Box 3965
San Francisco, CA 94119

Oak Ridge National Lab (4)
Attn: R. E. Blanko
E. Bondietti
C. Claiborne
G. H. Jenks
PO Box Y
Oak Ridge, TN 37830

Oak Ridge National Lab
Attn: John O. Blomeke
PO Box X
Oak Ridge, TN 37830

US Geological Survey
Water Resources Div
Attn: John D. Bredehoeft,
Western Region Hydrologist
345 Middlefield Rd
Menlo Park, CA 94025

Dr. Karl P. Cohen
928 N California Ave
Palo Alto, CA 94303

Stanford University
National Acad. of Sci., WIPP Panel
Dept. of Geology
Attn: Konrad B. Krauskopf, Chairman
Palo Alto, CA 94305

Vanderbilt University
Dept. of Environmental and
Water Resources Engineering
Attn: Frank L. Parker, Vice Chm.
Nashville, TN 37235

University of Florida
Department of Material Sciences and Engineering
Attn: Fred M. Ernsberger,
Adjunct Professor
Gainesville, FL 32611

Johns Hopkins University
Department of Earth Sciences
Attn: Hans P. Eugster
Baltimore, MD 21218

University of New Mexico
Department of Geology
Attn: Rodney C. Ewing
Albuquerque, NM 87131

University of Minnesota
Department of Geological Sciences
Attn: Charles Fairhurst
Minneapolis, MN 55455

University of Texas at Austin
Department of Geological Sciences
Attn: William R. Muehlberger
Austin, TX 78712

D'Arcy A. Shock
233 Virginia
Ponca City, OK 74601

National Academy of Sciences
Committee on Radioactive Waste Management
Attn: John T. Holloway, Senior Staff Officer
2101 Constitution Ave, NW
Washington, DC 20418

DISTRIBUTION (cont):

Hobbs Public Library
Attn: Marcia Lewis, Librarian
509 N. Ship St
Hobbs, NM 88248

NM Inst of Mining/Tech
Martin Speere Memorial Library
Campus St
Socorro, NM 87810

New Mexico State Library
Attn: Ingrid Vollenhofer
PO Box 1629
Santa Fe, NM 87503

University of New Mexico
Zimmerman Library
Attn: Zanier Vivian
Albuquerque, NM 87131

WIPP Public Reading Room
Attn: Gwynn Schreiner
Atomic Museum, Kirtland AFB, East
Albuquerque, NM 87185

WIPP Public Reading Room
Carlsbad Municipal Library
Attn: Lee Hubbard, Head Librarian
101 S Hallagueno St
Carlsbad, NM 88220

Thomas Brannigan Library
Attn: Don Dresp, Head Librarian
106 W Hadley St
Las Cruces, NM 88001

Roswell Public Library
Attn: Nancy Langston
301 N Pennsylvania Ave
Roswell, NM 88201

State of New Mexico (2)
Environmental Evaluation Group
Attn: Robert H. Neill, Dir
PO Box 968
Santa Fe, NM 87503

NM Department of Energy and Minerals (2)
Attn: Larry Kehoe, Secretary
Kasey LaPlante, Librarian
PO Box 2770
Santa Fe, NM 87501

Argonne National Lab (5)
Attn: S. Fried
A. M. Friedman
D. Hambeley
N. Meldgin
M. Steindler
9700 S Cass Ave
Argonne, IL 60439

Brookhaven National Lab (2)
Attn: P. Colombo, Dept of Applied Sciences
Cal Brewster, Bldg 830
Upton, NY 11973

Brookhaven National Lab
Associated Universities, Inc
Attn: Paul W. Levy, Senior Scientist
Upton, NY 11973

IT Corp (4)
Attn: P. Kelsall
R. McKinney
A. Moss
D. Shukla
Suite 306
2350 Alamo, SE
Albuquerque, NM 87106

E. I. Dupont de Nemours Co (4)
Attn: N. Bibler
E. J. Hennelly
M. J. Plodinec
G. G. Wicks
Savannah River Lab
Aiken, SC 29801

E. I. Dupont de Nemours Co
Attn: R. Baxter
Savannah River Plant
Aiken, SC 29801

Oak Ridge National Laboratory, Bldg. 2001
Ecological Sciences Information Center
Attn: C. S. Fore
PO Box X
Oak Ridge, TN 37830

Texas A&M University
Center of Tectonophysics
Attn: John Handin
College Station, TX 77840

DISTRIBUTION (cont):

J. F. T. Agapito Assoc, Inc
Attn: Christopher St. John
715 Horizon Dr, Suite 340
Grand Junction, CO 81501

Science Applications, Inc
Attn: D. E. Maxwell
2450 Washington Ave, Suite 120
San Leandro, CA 94577

Los Alamos National Lab
Attn: B. Erdal, CNC-11
PO Box 1663
Los Alamos, NM 87545

Rockwell International (3)
Atomics International Div
Attn: M. J. Smith
W. W. Schultz
P. Salter
Rockwell Hanford Operations
PO Box 800
Richland, WA 99352

US Department of Interior
Geological Survey
Attn: E. Roedder
959 National Center
Reston, VA 22092

Serata Geomechanics
Attn: Dr. Shosei Serata
4124 Lakeside Dr
Richmond, CA 94806-1941

Systems, Science, and Software (2)
Attn: P. Lagus
E. Peterson
Box 1620
La Jolla, CA 92038

Titanium Metals Corp of America
Henderson Technical Lab
Attn: R. W. Schulz
PO Box 2128
Henderson, NV 89015

US Army Engineers (8)
Waterways Experiment Station
Attn: D. Ainsworth
J. Armstrong
J. Boa
A. Buck
K. Mather
C. Pace
L. Wakeley
D. Walley
PO Box 631
Vicksburg, MS 39180

University of Arizona
Department of Mining
and Geological Engineering
Attn: J. J. K. Daemen
Tucson, AZ 85721

University of New Mexico
Geology Department
Attn: D. G. Brookins
Albuquerque, NM 87131

Cornell University
Department of Physics
Attn: Dr. R. O. Pohl
Clark Hall
Ithaca, NY 14853

Cornell University
Department of Mechanical
and Aerospace Engineering
Attn: Dr. Paul R. Dawson
254 Upson Hall
Ithaca, NY 14853

University of Minnesota
Department of Energy
and Materials Science
Attn: R. Oriani
151 Amundson Hall
421 Washington Ave, SE
Minneapolis, MN 55455

The Pennsylvania State University (2)
Materials Research Lab
Attn: Della Roy
Rustum Roy
University Park, PA 16802

DISTRIBUTION (cont):

Princeton University
Dept of Civil Engineering
Attn: George Pinder
Princeton, NJ 08540

RE/SPEC, Inc. (4)
Attn: P. Gnirk
T. Pfeifle
R. Stickney
L. Van Sambeek
PO Box 725
Rapid City, SD 57701

RE/SPEC, Inc (2)
Attn: S. W. Key
D. B. Blankenship
PO Box 14984
Albuquerque, NM 87191

Rockwell International (2)
Rocky Flats Plant
Attn: W. S. Bennett
C. E. Wickland
Golden, CO 80401

US Geological Survey
Special Projects
Attn: R. Snyder
MS954, Box 25046
Denver Federal Center
Denver, CO 80255

US Geological Survey
PO Box 26659
Albuquerque, NM 87125

Woodward-Clyde Consultants (2)
Library Western Region
Attn: Anne T. Harrigan, Librarian
Charles Taylor
3 Embarcadero Center, Suite 700
San Francisco, CA 94111

Institut fur Tieflagerung (3)
Attn: K. Kuhn
N. Jockwer
H. Gies
Theodor-Heuss-Strasse 4
D-3300 Braunschweig
FEDERAL REPUBLIC OF GERMANY

Bundesanstalt fur Geowissenschaften und Rohstoffe
Attn: Michael Langer
Postfach 510 153
3000 Hannover 51
FEDERAL REPUBLIC OF GERMANY

Hahn-Mietner-Institut fur Kernforschung
Attn: Klaus Eckart Maass
Glienicker Strasse 100
1000 Berlin 39
FEDERAL REPUBLIC OF GERMANY

Bundesministerium fur Forschung und Technologie
Attn: Rolf-Peter Randl
Postfach 200 706
5300 Bonn 2
FEDERAL REPUBLIC OF GERMANY

Physikalisch-Technische Bundesanstalt
Attn: Helmut Rothemeyer
Bundesanstalt 100
3300 Braunschweig
FEDERAL REPUBLIC OF GERMANY

Kernforschung Karlsruhe (3)
Attn: R. Koster
Reinhard Kraemer
K. D. Closs
Postfach 3640
7500 Karlsruhe
FEDERAL REPUBLIC OF GERMANY

Underground Storage of Radioactive Waste
Experimental Programs
Attn: Tuen Deboer, Manager
PO Box 1
1755 ZG Petten
THE NETHERLANDS

Svensk Karnbransleforsorjning AB
Project KBS
Karnbranslesakerhet
Attn: Fred Karlsson
Box 5864
10248 Stockholm
SWEDEN

Ontario Hydro Research Lab
Attn: Dr. D. K. Mukerjee
800 Kipling Ave
Toronto, Ontario
MBZ 554
CANADA

DISTRIBUTION (cont):

1510 J. W. Nunziato
1520 D. J. McCloskey
1521 R. D. Krieg
1521 H. S. Morgan
1540 W. C. Luth
1542 B. M. Butcher
1542 D. J. Holcomb
1542 L. W. Teufel
1542 W. R. Wawersik
1543 J. L. Krumhansl
1652 O. L. George, Jr.
1820 R. E. Whan
1830 M. J. Davis
1832 W. B. Jones
1832 J. W. Munford
1832 J. A. Van Den Avyle
1833 G. A. Knorovsky
1840 R. J. Eagan
1841 R. B. Diegle
1841 N. R. Sorensen
3310 W. D. Burnett
6000 E. H. Beckner
6253 D. A. Northrop
6253 A. R. Sattler
6257 R. R. Beasley
6257 J. K. Linn
6258 B. J. Thorne
6300 R. W. Lynch
6310 T. O. Hunter
6311 L. W. Scully
6312 F. W. Bingham
6314 J. R. Tillerson
6330 W. D. Weart
6331 A. R. Lappin
6331 G. E. Barr
6331 S. J. Lambert
6331 W. B. Miller
6331 K. L. Robinson
6331 S. E. Shaffer
6331 C. L. Stein (11)
6332 A. J. Arguello
6332 R. Beraun
6332 C. L. Christensen
6332 D. M. Ellett
6332 R. V. Matalucci
6332 M. A. Molecke
6332 D. E. Munson
6332 E. J. Nowak
6332 J. C. Stormont
6332 T. M. Torres
6332 L. D. Tyler (10)
6332 F. G. Yost
6332 Sandia WIPP Central Files (HLW) (2)
6334 L. H. Brush
7000 R. L. Peurifoy
7100 C. D. Broyles
7110 J. D. Plimpton
7112 C. R. Mehl
7112 G. H. Miller
7116 E. S. Ames
7116 C. W. Cook
7116 S. R. Dolce
7120 T. L. Pace
7125 J. T. McIlmoyle
7125 G. L. Ogle
7130 J. D. Kennedy
7133 C. W. Gulick
7133 R. D. Statler
7135 P. D. Seward
8310 R. W. Rohde
8314 N. R. Moody
8314 M. W. Perra
8314 S. L. Robinson
8315 D. H. Doughty
8315 L. A. West
8430 L. D. Bertholf
8024 M. A. Pound
3141 C. M. Ostrander (5)
3151 W. L. Garner (3)
3154-3 C. H. Dalin (28)
For DOE/TIC (Unlimited Release)